

Hydrodynamic turbulence cannot transport angular momentum effectively in astrophysical disks

Hantao Ji¹, Michael Burin¹†, Ethan Scharfman¹ & Jeremy Goodman¹

The most efficient energy sources known in the Universe are accretion disks. Those around black holes convert 5–40 per cent of rest-mass energy to radiation. Like water circling a drain, inflowing mass must lose angular momentum, presumably by vigorous turbulence in disks, which are essentially inviscid¹. The origin of the turbulence is unclear. Hot disks of electrically conducting plasma can become turbulent by way of the linear magnetorotational instability². Cool disks, such as the planet-forming disks of protostars, may be too poorly ionized for the magnetorotational instability to occur, and therefore essentially unmagnetized and linearly stable. Nonlinear hydrodynamic instability often occurs in linearly stable flows (for example, pipe flows) at sufficiently large Reynolds numbers. Although planet-forming disks have extreme Reynolds numbers, keplerian rotation enhances their linear hydrodynamic stability, so the question of whether they can be turbulent and thereby transport angular momentum effectively is controversial^{3–15}. Here we report a laboratory experiment, demonstrating that non-magnetic quasi-keplerian flows at Reynolds numbers up to millions are essentially steady. Scaled to accretion disks, rates of angular momentum transport lie far below astrophysical requirements. By ruling out purely hydrodynamic turbulence, our results indirectly support the magnetorotational instability as the likely cause of turbulence, even in cool disks.

Our experiments involved a novel Taylor–Couette apparatus¹⁶. The rotating liquid (water or a water/glycerol mixture) is confined between two concentric cylinders of radii r_1 , r_2 ($r_2 > r_1$) and height h . The angular velocity of the fluid is controlled by that of the cylinders, Ω_1 and Ω_2 . An infinitely long, steady, Taylor–Couette flow rotates as:

$$\Omega(r) = a + \frac{b}{r^2} \quad (1)$$

where $a = (\Omega_2 r_2^2 - \Omega_1 r_1^2) / (r_2^2 - r_1^2)$ and $b = r_1^2 r_2^2 (\Omega_1 - \Omega_2) / (r_2^2 - r_1^2)$. Reynolds number here can be defined as $\bar{r}(r_2 - r_1)(\Omega_1 - \Omega_2) / \nu$, where ν is viscosity and $\bar{r} \equiv (r_1 + r_2) / 2$. The rotation profile (equation (1)) ensures a radially constant viscous torque $-2\pi\rho\nu h r^3 \partial\Omega / \partial r$ for constant mass density ρ and constant ν . Astrophysical disks are mostly keplerian, meaning $\Omega \propto r^{-3/2}$, so that $|\Omega|$ decreases radially outward ($\partial|\Omega| / \partial r < 0$) while the specific angular momentum, $|r^2\Omega|$, increases radially ($\partial|r^2\Omega| / \partial r > 0$). We apply the term ‘quasi-keplerian’ to any flow satisfying these conditions, which are crucial for both hydrodynamic and magnetohydrodynamic linear stability⁷.

Real flows have finite length. Disks have nearly stress-free vertical boundaries, but viscous stress at the vertical endcaps of laboratory flows drives secondary circulation. This may cause the rotation profile to deviate significantly from equation (1), and may even provoke turbulence^{7,15,17–20}. Our apparatus incorporates two rings at each end that are driven independently of the cylinders (Fig. 1). Thus we have four controllable angular velocities. When we choose these

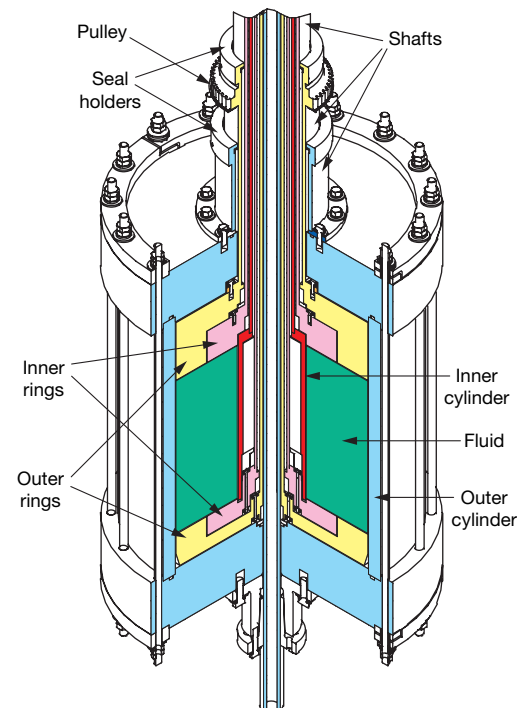


Figure 1 | Experimental set-up. A rotating fluid (water or a water/glycerol mixture) of height $h = 27.86$ cm is confined between two concentric cylinders of radii $r_1 = 7.06$ cm and $r_2 = 20.30$ cm, which rotate at rates of Ω_1 and Ω_2 , respectively. Two novel features distinguish this apparatus from conventional Taylor–Couette experiments. First, secondary circulation is controlled by dividing each endcap into two independently driven rings. Opposing rings at top and bottom are driven at the same selectable angular velocity Ω_3 (inner rings) and Ω_4 (outer rings). Traditionally, a large aspect ratio $\Gamma \equiv h / (r_2 - r_1)$ is used to reduce the secondary circulation. However, at $\Gamma \approx 25$ by Richard⁷ and even at $\Gamma \approx 100$ by Taylor¹⁸, end effects were reported to be significant when the endcaps co-rotated with one of the cylinders. Even when the endcaps were divided into two rings, but with each affixed to one cylinder^{7,17}, residual secondary circulation may have facilitated the observed turbulent transition^{15,19}. When Ω_3 and Ω_4 are appropriately chosen, secondary circulation is minimized and ideal Couette profiles are well approximated²¹. A second novel feature is access to rotation profiles on both sides of marginal linear stability at Reynolds numbers as large as 10^6 (see also Fig. 2). When the specific angular momentum, $|r^2\Omega|$, decreases with increasing r , the Rayleigh stability criterion³⁰ is violated, and thus the flow is linearly unstable when the Reynolds number exceeds a critical value¹⁶. When $\partial|r^2\Omega| / \partial r > 0$ but $\partial|\Omega| / \partial r < 0$ (as in disks, where $\Omega \propto r^{-3/2}$), the flow is quasi-keplerian and known to be linearly stable to axisymmetric disturbances. All major components of the apparatus were precisely machined and balanced, and except for the inner cylinder and rotating shafts, are made of clear acrylic to facilitate visual and laser diagnostics.

¹Center for Magnetic Self-organization in Laboratory and Astrophysical Plasmas, Plasma Physics Laboratory and Department of Astrophysical Sciences, Princeton University, Princeton, New Jersey 08543, USA. †Present address: Department of Physics and Astronomy, Pomona College, Claremont, California 91711, USA.

appropriately, secondary circulation is minimized, and ideal Couette profiles are closely approximated throughout the flow, except within ~ 1 cm of the endcaps²¹.

Most past work has taken the outer cylinder at rest ($\Omega_2 = 0$), so that both $|\Omega|$ and $|r^2\Omega|$ decrease radially outward. Such flows are axisymmetrically linearly unstable¹⁶ at modest Reynolds number, Re . Very few experiments have studied the linearly stable regime where $\partial|r^2\Omega|/\partial r > 0$, as occurs in disks. Among these few are two classic experiments of the 1930s: in one of these, the inner cylinder was at rest ($\Omega_1 = 0$)¹⁸, while in the other¹⁷, $0 \leq \Omega_1/\Omega_2 \leq 1$. Enhanced torques between the cylinders and other evidence of turbulence were reported at sufficiently large Re . These results have been cited in support of the hypothesis of nonlinear hydrodynamic turbulent transport in disks^{3,6}, notwithstanding that the direction of turbulent angular momentum transport, which always follows $-\partial\Omega/\partial r$ on energetic grounds, differs in sign between these experiments and astrophysical disks. The so-called β prescription⁶ derived from the above experiments has been used to model or interpret astronomical observations²². To our knowledge, the only published experiments with quasi-keplerian flow at relevant Reynolds numbers are those of Richard^{7,14} and Beckley²³. In Richard's work, transition to turbulence via nonlinear instabilities was studied qualitatively by a flow-visualization method. No direct measurements of angular momentum transport were performed. Beckley did measure torques roughly

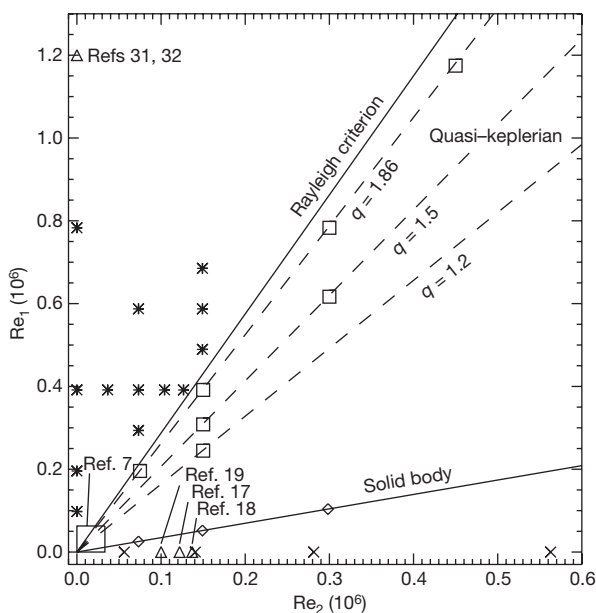


Figure 2 | Experimentally studied Taylor-Couette flows. Axes are Reynolds numbers based on the inner and outer cylinders: $Re_{1,2} \equiv \Omega_{1,2} r_{1,2} (r_2 - r_1) / \nu$. Asterisks mark Rayleigh-unstable flows; squares, quasi-keplerian ones, that is $\partial|\Omega|/\partial r < 0$ but $\partial|r^2\Omega|/\partial r > 0$; diamonds, solid-body flows ($\partial\Omega/\partial r = 0$); crosses for the inner cylinder at rest; triangles for flows explored in previous experiments^{17–19,31,32}; and the rectangular box for the parameter regime explored by Richard⁷. Dashed lines denote constant values of $q \equiv -\partial \ln \Omega / \partial \ln r$ at $r = 17$ cm, where most of our measurements of Reynolds stress were performed (Fig. 3). Rayleigh-unstable flows exhibit 5–10% fluctuations that are insensitive to the end-ring speeds. Quasi-keplerian and other Rayleigh-stable flows are more sensitive. For example, when the end-rings speeds are fixed to the cylinders, fluctuations up to 4–8% occur. When the end-ring speeds are adjusted so that the ideal-Couette profile is restored, fluctuations are 1–2% and indistinguishable from those of our solid-body flows, except within a few cm of the boundary. Reducing Re by a factor of $\sim 1/18$, using an admixture of glycerol, actually increases the fluctuation level for the same (nearly ideal-Couette) profile. We interpret this to mean that the residual unsteady secondary circulation penetrates deeper into the bulk flow at lower Re . We infer from this that the experiments by Richard⁷ may have been affected by the endcaps, although his ratio of height to gap width exceeded ours. His endcaps were split but fixed to the cylinders.

consistent with the β prescription, but attributed them to secondary circulation, which was strong because the endcaps of his apparatus co-rotated with the outer cylinder and $h/(r_2 - r_1)$ was only ~ 2 .

Experimental flows studied by ourselves and others are summarized in Fig. 2. Our Reynolds numbers are up to 20 times larger than those previously achieved by Richard⁷. A laser Doppler velocimetry (LDV) system was used to sample the azimuthal velocity v_θ at various radial and axial locations. Both mean values, $\bar{v}_\theta \equiv r\Omega$, and fluctuations, $v'_\theta \equiv v_\theta - \bar{v}_\theta$, were obtained. At our Reynolds numbers, linearly-unstable flows are always turbulent, with fluctuation levels $(\overline{v'^2_\theta})^{1/2} / \bar{v}_\theta = 5 - 10\%$. They are largely insensitive to the endcap speeds. In contrast, quasi-keplerian and other linearly-stable flows are sensitive to the endcap boundary conditions. When the endcap speeds are adjusted to best approximate ideal Couette flow, the fluctuations are 1–2% and indistinguishable from those of our solid-body flows, which are expected to be steady or laminar owing to the lack of shear to drive turbulence.

One hallmark of nonlinear instability is hysteresis: the transition from laminar flow to turbulence occurs at higher Reynolds numbers than the reverse⁷. Quiescent flows were gradually brought into linearly-unstable regimes by raising Ω_1 or lowering Ω_2 , then returned to linearly-stable regimes. Significant fluctuations were found only in the linearly-unstable regime; no hysteresis was detected.

In the absence of magnetic fields, turbulent angular momentum transport requires correlated velocity fluctuations. The radial angular momentum flux is $\rho r \overline{v'_\theta v'_r}$, where v'_r is the fluctuation in radial velocity, and the turbulent viscosity ν_{turb} is defined by equating this to $-\rho \nu_{\text{turb}} r^2 \partial\Omega/\partial r$ where $\nu_{\text{turb}} = \beta |r^2 \partial\Omega/\partial r|$, so that $\beta = \overline{v'_\theta v'_r} / (r^2 \partial\Omega/\partial r)^2$ is dimensionless. Conveniently, in a turbulent but statistically steady state with a profile given by equation (1), both β and ν_{turb} are radially constant. A value of $\beta = (1-2) \times 10^{-5}$ has been deduced⁶ from experiments^{17,18} with $0 \leq \Omega_1/\Omega_2 < 1$.

We have measured the Reynolds stress directly using a synchronized dual-LDV system. Both v'_θ and v'_r appear to follow gaussian statistics (E.S. *et al.*, manuscript in preparation), and random errors

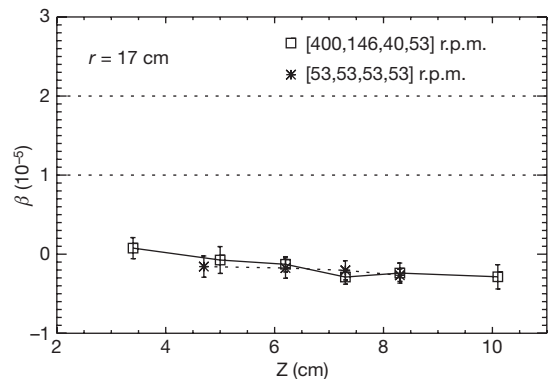


Figure 3 | Experimentally measured Reynolds stress versus height in a quasi-keplerian profile. Here $\beta \equiv \overline{v'_\theta v'_r} / (\overline{v'^2_\theta} q^2)$ sign ($q\Omega$), where $q \equiv -\partial \ln \Omega / \partial \ln r$: $q = +3/2$ in keplerian disks, $1.2 \leq q \leq 1.9$ in our quasi-keplerian flows. Square symbols connected by a solid line were taken at $q = 1.86$ (see Fig. 2). Starred points connected by a dotted line are a solid-body case ($q = 0$), which should be non-turbulent and therefore serves as a control for systematic errors. The measured values fall far below the range of β proposed by Richard and Zahn⁶, shown with horizontal dotted lines. The measurements were performed using a synchronized, dual laser-Doppler-velocimetry (LDV) system, which allows simultaneous detection of both components of velocity v_θ and v_r . The laser beams enter the fluid vertically through the acrylic endcaps from below (see Fig. 1), and Z is the height above the lower endcap. Rotation speeds $[\Omega_1, \Omega_3, \Omega_4, \Omega_2]$ are shown, where Ω_3 and Ω_4 are the angular velocities of the inner and outer end-rings. Apparently gaussian deviations amounting to $\sim (1-2\%)$ of \bar{v}_θ were observed from sample to sample, representing measurement errors and perhaps true fluctuations. Each data point is the mean of β computed from 3,000–10,000 samples. Error bars represent the standard deviations.

were reduced by averaging 10^3 – 10^4 samples. Systematic errors were gauged by comparison with solid body flows ($\Omega_1 = \Omega_2 = \Omega_3 = \Omega_4$). Figure 3 shows that β differs indistinguishably between quasi-keplerian and solid-body rotation, falling far below the proposed range⁶. A large outward Reynolds stress is detected in linearly-unstable flows, $\beta > 10^{-3}$, as expected (M.B. *et al.*, manuscript in preparation). Even for linearly-stable flows, when the speeds (Ω_3, Ω_4) of the endcaps were not adjusted properly to produce the ideal Couette profile of equation (1), β was found to be almost 10^{-4} (Fig. 4). This again indicates that the axial boundaries can profoundly influence linearly-stable flows, as previously suggested^{15,19}.

A final point should be made about the critical Reynolds number for transition, Re_{crit} , versus gap width. Based on the experiments reported in refs 17 and 18, the scaling $Re_{crit} \approx 6 \times 10^5 [(r_2 - r_1)/\bar{r}]^2$ has been proposed^{3,4,6,8}. It is unclear whether this scaling applies to quasi-keplerian flow as it was derived from data for $\Omega_2/\Omega_1 > 1$. In any case, up to $Re = 2 \times 10^6$, which is about three times the proposed

Re_{crit} because $(r_2 - r_1)/\bar{r} \approx 1$ in our device, we have seen no signs of rising fluctuation levels or Reynolds stress (Fig. 4).

Therefore, we have shown that purely hydrodynamic quasi-keplerian flows, under proper boundary conditions and at large enough Reynolds numbers, cannot transport angular momentum at astrophysically relevant rates.

Of course, it could be argued that our maximum Re , which only barely exceeds some theoretical estimates¹³ of Re_{crit} , is still not large enough for transition. Or it could be that transition has occurred, but that the transport is too small for us to detect. To extrapolate from $Re \leq 2 \times 10^6$ to a typical astrophysical value $\geq 10^{12}$, we rely on the empirical observation that for $Re > Re_{crit}$, the Reynolds number based on the turbulent rather than the molecular viscosity is approximately independent of Re itself. It follows that $v_{turb} \approx LU/Re_{crit}$ for $Re > Re_{crit}$, where L and U are the characteristic size and velocity of the flow. It is common knowledge among civil engineers that this is true of flow in pipes, for example²⁴. If it is true of rotating shear flow, as theoretical arguments suggest it should be¹⁵, then β at $Re \geq 10^{12}$ should be comparable to what we find at $Re \leq 2 \times 10^6$, namely, $\beta < 6.2 \times 10^{-6}$ (at 2 s.d., or 98% confidence; see Fig. 4 legend)—whether or not we have crossed the threshold of transition.

Lastly, it is useful to relate the above upper bound for β to the more commonly used Shakura–Sunyaev α parameter¹: $v_{turb} = \alpha \Omega h^2$. We replace this by $v_{turb} = \alpha \Omega (r_2 - r_1)^2$ since $r_2 - r_1$ is smaller than h in our experiment, and we presume that the dominant turbulent eddies scale with the smallest dimension of the flow ($h \ll r$ in most disks). Then $\alpha = \beta q \bar{r}^2 / (r_2 - r_1)^2 \approx \beta q$ (see Fig. 3 legend for a definition of q), and thus our results imply a similar upper bound for α as for β in purely hydrodynamic disks, whereas protostellar-disk lifetimes and accretion rates indicate²⁵ $\alpha \geq 10^{-3}$. Although it has been suggested that complications such as vertical or radial stratification may yet lead to essentially linear non-axisymmetric hydrodynamic instabilities^{26,27}, our belief is that such non-axisymmetric linear instabilities depend upon radial boundaries and hence are not generally important in thin disks^{28,29}. If this is correct, then by default, the magnetorotational instability appears to be the only plausible source of accretion disk turbulence.

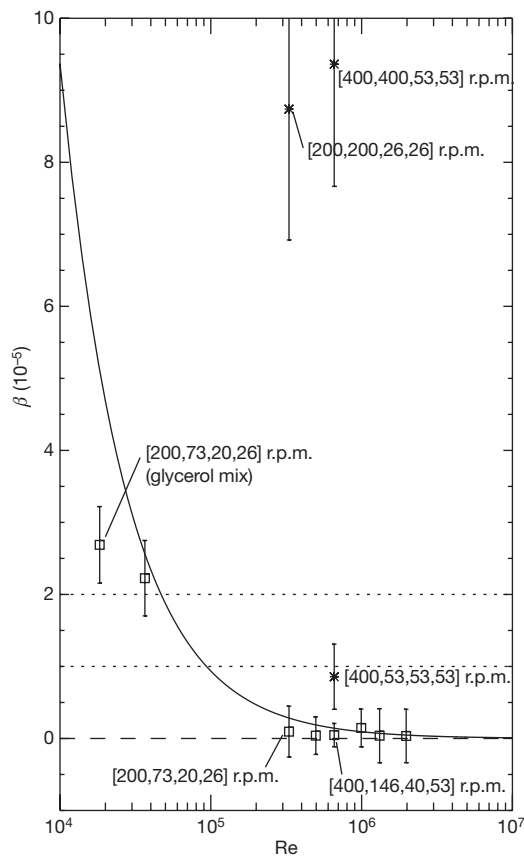


Figure 4 | Dimensionless Reynolds stress at Reynolds numbers up to 2×10^6 . At the largest Re , the data show no sign that $\beta \equiv v_0' v_r' / (\overline{v_0'}^2 q^2)$ or the relative fluctuations $v^2 / (\overline{v_0'})^2$ themselves increase with Re in quasi-keplerian flows. Here $q \equiv -\partial \ln \Omega / \partial \ln r$ is calculated from the mean $v_0(r)$ profiles. Systematic errors in β have been removed by reference to identical measurements in solid-body flows. Different sizes of error bars (showing s.d.) for the six quasi-keplerian flows with optimum boundary conditions (squares at $Re > 10^5$) are largely due to different numbers of measurement samples, N . Averaging over these 6 points, weighted by \sqrt{N} , results in $\beta = 0.72 \times 10^{-6}$ with s.d. of 2.7×10^{-6} or $\beta < 6.2 \times 10^{-6}$ at 2 s.d. (98% confidence). When the end-ring speeds are not optimized to produce Couette profiles (equation (1)), however, β exhibits large values (asterisks). When optimal speeds are used but glycerol is added to the water to reduce the Reynolds number, larger β values are also seen (squares at $Re < 10^5$), possibly due to stronger residual secondary circulation. For reference, the solid line is the molecular viscous value: $\beta_{visc} \equiv v / [\bar{r}^3 (\Omega_2 - \Omega_1) / (r_2 - r_1)] = Re^{-1} (r_2 - r_1)^2 / \bar{r}^2$. The proposed β lies between the horizontal dotted lines⁶.

Received 8 August; accepted 6 October 2006.

- Shakura, N. I. & Sunyaev, R. A. Black holes in binary systems. Observational appearance. *Astron. Astrophys.* **24**, 337–355 (1973).
- Balbus, S. A. & Hawley, J. F. Instability, turbulence, and enhanced transport in accretion disks. *Rev. Mod. Phys.* **70**, 1–53 (1998).
- Zeldovich, Y. B. On the friction of fluids between rotating cylinders. *Proc. R. Soc. Lond. A* **374**, 299–312 (1981).
- Dubrulle, B. Differential rotation as a source of angular momentum transfer in the solar nebula. *Icarus* **106**, 59–76 (1993).
- Balbus, S. A., Hawley, J. F. & Stone, J. M. Nonlinear stability, hydrodynamical turbulence, and transport in disks. *Astrophys. J.* **467**, 76–86 (1996).
- Richard, D. & Zahn, J.-P. Turbulence in differentially rotating flows: What can be learned from the Couette–Taylor experiment. *Astron. Astrophys.* **347**, 734–738 (1999).
- Richard, D. *Instabilités Hydrodynamiques dans les Ecoulements en Rotation Différentielle*. Ph.D. thesis, Univ. Paris 7 (2001).
- Longaretti, P. On the phenomenology of hydrodynamic shear turbulence. *Astrophys. J.* **576**, 587–598 (2002).
- Chagelishvili, G. D., Zahn, J.-P., Tevzadze, A. G. & Lominadze, J. G. On hydrodynamic shear turbulence in Keplerian disks: Via transient growth to bypass transition. *Astron. Astrophys.* **402**, 401–407 (2003).
- Yecko, P. A. Accretion disk instability revisited. Transient dynamics of rotating shear flow. *Astron. Astrophys.* **425**, 385–393 (2004).
- Umurhan, O. M. & Regev, O. Hydrodynamic stability of rotationally supported flows: Linear and nonlinear 2D shearing box results. *Astron. Astrophys.* **427**, 855–872 (2004).
- Garaud, P. & Ogilvie, G. I. A model for the nonlinear dynamics of turbulent shear flows. *J. Fluid Mech.* **530**, 145–176 (2005).
- Mukhopadhyay, B., Afshordi, N. & Narayan, R. Bypass to turbulence in hydrodynamic accretion disks: An eigenvalue approach. *Astrophys. J.* **629**, 383–396 (2005).
- Dubrulle, B. *et al.* Stability and turbulent transport in Taylor–Couette flow from analysis of experimental data. *Phys. Fluids* **17**, 095103, doi:10.1063/1.2008999 (2005).

15. Lesur, G. & Longaretti, P.-Y. On the relevance of subcritical hydrodynamic turbulence to accretion disk transport. *Astron. Astrophys.* **444**, 25–44 (2005).
16. Taylor, G. I. Stability of a viscous liquid contained between two rotating cylinders. *Phil. Trans. R. Soc. Lond. A* **223**, 289–343 (1923).
17. Wendt, F. Turbulente Strömungen zwischen zwei rotierenden konaxialen Zylindern. *Ing. Arch.* **4**, 577–595 (1933).
18. Taylor, G. I. Fluid friction between rotating cylinders. i. torque measurements. *Proc. R. Soc. Lond. A* **157**, 546–578 (1936).
19. Schultz-Grunow, F. Zur Stabilität der Couette-Strömung. *Z. Angew. Math. Mech.* **39**, 101–117 (1959).
20. Kageyama, A., Ji, H., Goodman, J., Chen, F. & Shoshan, E. Numerical and experimental investigation of circulation in short cylinders. *J. Phys. Soc. Jpn* **73**, 2424–2437 (2004).
21. Burin, M. J. *et al.* Reduction of Ekman circulation within a short circular couette flow. *Exp. Fluids* **40**, 962–966, doi:10.1007/s00348-006-0132-y (2006).
22. Hueso, R. & Guillot, T. Evolution of protoplanetary disks: constraints from DM Tauri and GM Aurigae. *Astron. Astrophys.* **442**, 703–725 (2005).
23. Beckley, H. *Measurements of Annular Couette Flow Stability at the Fluid Reynolds Number $Re = 4.4 \times 10^6$: The Fluid Dynamic Precursor to a Liquid Sodium $\alpha\omega$ Dynamo.* PhD thesis, New Mexico Inst. Mining Technol. (2002).
24. Colebrook, C. F. Turbulent flow in pipes with particular reference to the transitional region between smooth and rough pipes. *J. Inst. Civil Eng.* **11**, 133–156 (1938).
25. Hartmann, L., Calvet, N., Gullbring, E. & D’Alessio, P. Accretion and the evolution of T Tauri disks. *Astrophys. J.* **495**, 385–400 (1998).
26. Klahr, H. H. & Bodenheimer, P. Turbulence in accretion disks: Vorticity generation and angular momentum transport via the global baroclinic instability. *Astrophys. J.* **582**, 869–892 (2003).
27. Dubrulle, B. *et al.* An hydrodynamic shear instability in stratified disks. *Astron. Astrophys.* **429**, 1–13 (2005).
28. Johnson, B. M. & Gammie, C. F. Nonlinear stability of thin, radially-stratified disks. *Astrophys. J.* **636**, 63–74 (2006).
29. Goodman, J. & Balbus, S. A. Stratified disks are locally stable. Preprint at (<http://arxiv.org/astro-ph/0110229>) (2001).
30. Rayleigh, Lord On the dynamics of rotating fluid. *Proc. R. Soc. Lond. A* **93**, 148–154 (1916).
31. Lathrop, D. P., Fineberg, J. & Swinney, H. L. Turbulent flow between concentric rotating cylinders at large Reynolds number. *Phys. Rev. Lett.* **68**, 1515–1518 (1992).
32. Lewis, G. S. & Swinney, H. L. Velocity structure functions, scaling, and transitions in high-Reynolds-number Couette-Taylor flow. *Phys. Rev. E* **59**, 5457–5467 (1999).

Acknowledgements We thank S. Balbus for discussions, R. Cutler for technical assistance with the apparatus, P. Heitzenroeder, C. Jun, L. Morris and S. Raftopolous for engineering assistance, as well as Dantec Dynamics for the contracted use of an LDV measurement system. This research was supported by the US Department of Energy, Office of Science – Fusion Energy Sciences Program; the US National Aeronautics and Space Administration, Astronomy and Physics Research and Analysis and Astrophysics Theory Programs; and the US National Science Foundation, Physics and Astronomical Sciences Divisions.

Author Contributions H.J., M.B. and E.S. planned and executed the experiments, and analysed data; E.S. and M.B. prepared apparatus and diagnostics; H.J. drafted the paper; and J.G. suggested this subject and assisted in the interpretation of the results and in revising the paper.

Author Information Reprints and permissions information is available at www.nature.com/reprints. The authors declare no competing financial interests. Correspondence and requests for materials should be addressed to H.J. (hji@pppl.gov).